Journal of Hepatocellular Carcinoma

Dovepress
open access to scientific and medical research

Open Access Full Text Article

ORIGINAL RESEARCH

Prognosis of Primary Liver Cancer Based on LI-RADS Classification with Extracellular Agent-Enhanced MRI

Yubo Li[1–4], Xiaoyan Ni[2–4], Xinai Liu[1], Chun Yang[2–4], Yi Wang[2,4], Xin Lu[2–4], Changwu Zhou[2–4]

[1]Department of MRI, Henan Provincial Hospital of Traditional Chinese Medicine (the Second Affiliated Hospital of Henan University of Traditional Chinese Medicine), Zhengzhou, People's Republic of China; [2]Department of Radiology, Zhongshan Hospital, Fudan University, Shanghai, People's Republic of China; [3]Shanghai Institute of Medical Imaging, Shanghai, People's Republic of China; [4]Department of Cancer Center, Zhongshan Hospital, Fudan University, Shanghai, People's Republic of China

Correspondence: Xin Lu; Changwu Zhou, Shanghai Institute of Medical Imaging; Department of Radiology, Zhongshan Hospital, Fudan University, No. 180 Fenglin Road, Xuhui District, Shanghai, 200032, People's Republic of China, Tel +86 18702135336; +86 13912121145, Email luxcn@163.com; changwu83@163.com

Objective: The prognostic value of the Liver Imaging Reporting and Data System (LI-RADS) 2018 in differentiating hepatocellular carcinoma (HCC) from other primary liver cancers (PLC) with cirrhosis is unclear. We aim to evaluate the value of LI-RADS 2018 with agent-enhanced MRI in the postoperative prognosis of PLC patients with cirrhosis.

Methods: Between 2016 and 2021, 432 patients with cirrhosis and surgically proven single primary liver cancer were retrospectively evaluated. Two radiologists evaluated the preoperative MRI features independently and assigned each lesion a LI-RADS category. Overall survival (OS), recurrence-free survival (RFS), and their associated factors were evaluated by using the Kaplan-Meier method, Log rank test, and Cox proportional hazards model.

Results: The mean age of 432 patients (239 HCCs, 93 ICCs, and 100 cHCC-CCAs) was 57.27±10.92 years. The LR-M category showed poorer OS and RFS than the LR-4 or LR-5 category did for all primary liver cancers ($P < 0.001$ for both), and so did HCCs with tumor size less than 30mm ($P = 0.003$ and $P = 0.04$, respectively). In the multivariable analysis, the LI-RADS category and tumor size > 30 mm had independent correlations with OS and RFS (all $P < 0.05$). Multivariable Cox analysis identified rim arterial phase hyperenhancement (APHE) as independent determinants of poor OS and RFS in primary liver cancers (all $P < 0.05$).

Conclusion: The LI-RADS categories can predict the postsurgical prognosis of primary liver cancers independently.

Keywords: hepatocellular carcinoma, magnetic resonance imaging, prognosis, liver cirrhosis

Introduction

Primary liver cancer (PLC), as the fourth most common malignancy and one of the main causes of morbidity and mortality in patients with liver cirrhosis,[1–3] is mainly divided into hepatocellular carcinoma (HCC), intrahepatic cholangiocarcinoma (iCCA) and combined hepatocellular carcinoma-cholangiocarcinoma (cHCC-CCA) according to pathological types. Compared with iCCA and cHCC-CCA, HCC can be diagnosed according to stringent imaging criteria in high-risk patients without invasive confirmatory testing.[4–6] These three types of PLC vary greatly in prognosis and treatment methods,[7,8] when risk factors overlap, the accurate differentiation between non-HCC malignancies and HCC in patients with cirrhosis is especially important.[4]

The Liver Imaging Reporting and Data System (LI-RADS) which standardizes imaging for the diagnosis of HCC, has updated in 2018 and achieved consistency with the American Association for the Study of Liver Diseases (AASLD) 2018 HCC clinical practice guidance by revising the criterion for small (10–19 mm) observations in LR-5 category and modifying the definition for threshold growth.[2,3,9]

Currently, most recent validation studies have focused on the evaluation of the LI-RADS with gadoxetate disodium,[4,10,11] and the use of the old category of cHCC-CCA according to 2010 WHO classification system. Some

Received: 4 November 2022
Accepted: 20 February 2023
Published: 9 March 2023

researchers believe that the results with gadoxetate disodium are controversial.[4,12,13] As we all known, the magnetic resonance extracellular contrast agents (ECA) are distributed throughout the extracellular fluid compartments with bolus injection, producing contrast enhancement of the liver parenchyma and liver tumors.[14] Most of the current research demonstrated that hepatobiliary agents (HBA) affected the enhancement effect in the arterial phase of various tumors, especially of hypervascular tumors such as hepatocellular carcinoma and renal cell carcinoma.[14,15] Min et al[16] indicated that washout is more perceptible in the delayed phase than in the portal venous phase. Additionally, the phenomenon of transient dyspnea has also been thought to attribute to lower-quality arterial phase imaging with gadoxetate.[17]

The prognostic value of the LI-RADS classification with extracellular agents according to the 2018 LI-RADS criterion[9] for differentiating HCC from PLCs that meet 2019 WHO classification criterion has yet to be determined. A previous study distinguished high-risk factors associated with the recurrence of cHCC-CCAs according to the LI-RADS classification.[18] The generalization of the results may be different when applied to PLC.

Therefore, we aim to evaluate the value of LI-RADS 2018 with extracellular agent-enhanced MRI in the post-operative prognosis of PLC patients with cirrhosis and identify the general prognostic risk factors among the imaging features of LI-RADS.

Materials and Methods

Patients

Our study complied with the Declaration of Helsinki. This retrospective study was approved by the Institutional Review Board of Zhongshan Hospital, Fudan University (Approval Number: B2021-325R), and written informed consent was required from all of the patients before enrollment. We retrospectively identified 3850 patients who were confirmed to have PLCs after surgery in our institution between January 2016 and November 2021. The eligible patients were consecutively enrolled in our study. Inclusion criteria were as follows: a) patients pathologically proven single HCC, ICC or cHCC-CCA; b) enhanced MRI performed with extracellular contrast agents within 1 month of liver surgery; c) histopathologic confirmation of liver cirrhosis; and d) no prior history of antitumor treatment before liver surgery. Exclusion criteria were as follows: a) inadequacy of imaging for analysis due to severe motion artifact; b) patients with cirrhosis due to chronic portal vein occlusion (caused by schistosome); c) lost to follow up. They all had Child–Pugh class A cirrhosis. The flow chart of patient enrollment is shown in Figure 1. Ultimately, 432 patients were enrolled, including 239 HCC, 93 iCCA and 100 cHCC-CCA patients.

Clinical Data Evaluation

The clinical data of the patients, including hepatitis B/C virus infection status, age, sex, serum tumor markers level - alpha-fetoprotein (AFP), carcinoembryonic antigen (CEA) and carbohydrate antigen 19–9 (CA19-9) within 7 days before surgery, were retrospectively analyzed. Accordingly, AFP, CEA, and CA19-9 cutoff values were 20ng/mL, 5ng/mL, and 37ng/mL, respectively.

MRI Technique

A 1.5-T MRI scanner (uMR 560, United Imaging Healthcare) with a 24-channel body array coil was used to scan all patients. Routine liver protocols consisted of transverse T1-weighted imaging (T1WI) breath-hold in-phase and opposed-phase sequences, T2WI with fat-suppressed, diffusion-weighted imaging (DWI, b value = 0, 50, and 500 s/mm2) and enhanced T1WI with fat-suppressed breath-hold sequence. At a rate of 2mL/s, 0.1 mmol/kg of contrast agent (gadolinium diethylenetriamine pentaacetic acid, Gd-DTPA; Magnevist, Bayer HealthCare) was administered into the vein to obtain the arterial phase at 10–14 s, the portal venous phase at 70–90 s and delayed phase at 160–180 s, respectively.

MRI Analysis

Two abdominal radiologists (with 12 and 14 years of experience, respectively) who were blinded to the pathologic results, analyzed all imaging sequences and assigned each lesion with a LI-RADS category independently. According to the presence or absence of LI-RADS features, nodules were classified as category ranged from LR-3 (intermediate

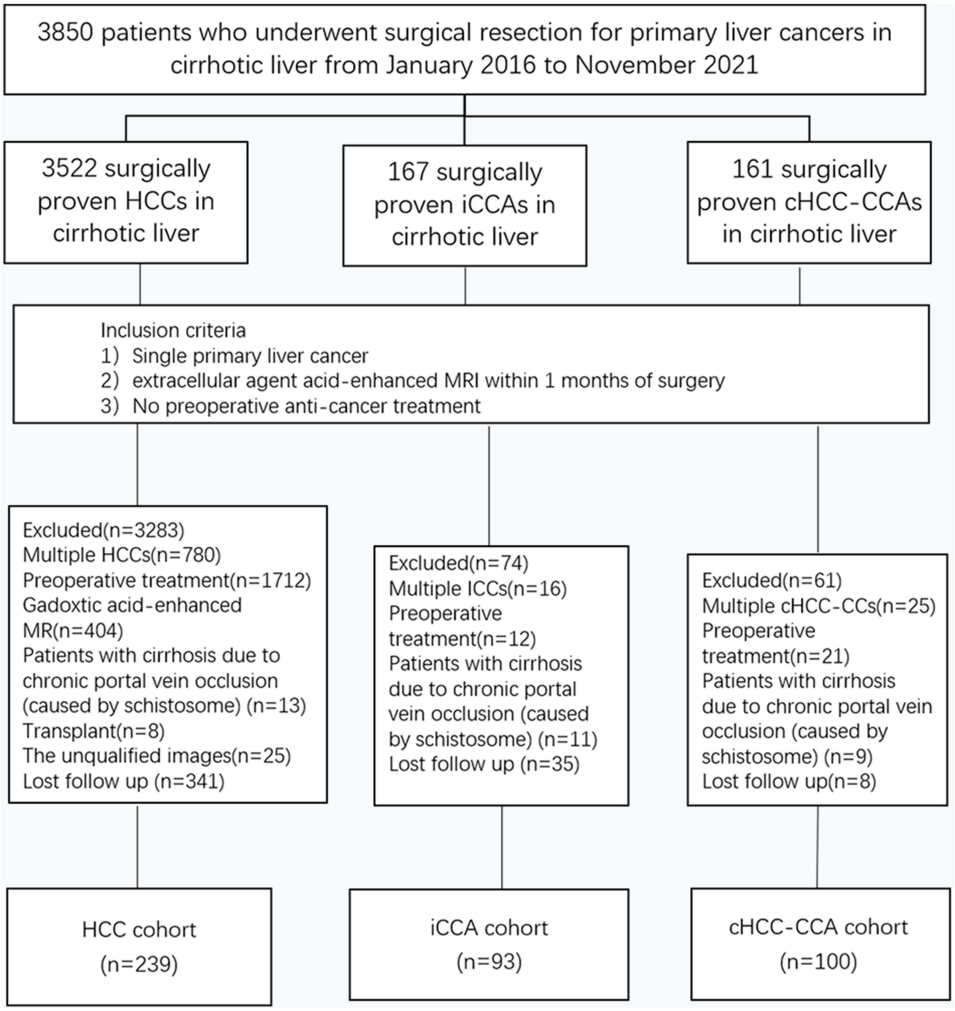

Figure 1 Flowchart of the study cohort.
Abbreviations: HCC, hepatocellular carcinoma; iCCA, intrahepatic cholangiocarcinoma; cHCC-CCA, combined hepatocellular carcinoma-cholangiocarcinoma.

probability of HCC) to LR-5 (definitely HCC), LR-M (probably malignant, not specific for HCC), or LR-TIV (definitely tumor in the vein). As these patients had only one preoperative MRI, threshold growth was excluded. In case of disagreement, the two observers had access to a consensus by discussion. In this study, the two radiologists evaluated nodule size, location, and the presence or absence of imaging features. A total of 16 imaging features were evaluated, including LI-RADS 2018[9] all major features, targetoid mass features, ancillary features and additional ancillary features (particularly prone to malignancy) which was mentioned in the available literature.[19–21]

The imaging features were as follows: a) non-rim arterial phase hyperenhancement (APHE); b) nonperipheral washout; c) enhancing capsule; d) rim APHE; e) peripheral washout; f) delayed central enhancement; g) targetoid restriction; h) nodule-in-nodule; i) mosaic architecture; j) fat in mass, more than adjacent liver; k) blood products in mass; l) restricted diffusion; m) mild-moderate T2 hyperintensity; n) corona enhancement; o) peritumoral biliary dilatation; and p) liver surface retraction.

Histopathologic Analysis

The histopathologic diagnoses of hepatic nodules were made according to the updated 2019 WHO classification[22] on the basis of morphologic features on hematoxylin-eosin–stained slices and immunohistochemistry analysis, such as alpha-fetoprotein, polyclonal carcinoembryonic antigen, hepatocyte paraffin 1, cytokeratin-7, cytokeratin-19, CD56, and CD117. In addition, morphologically typical HCCs or CCAs with only immunohistochemical expression of stem cell

markers are not considered as a biphenotypic PLC, but rather as HCCs or CCAs. In addition to tumor diagnosis, the presence of macro- or microvascular tumor invasion was assessed.

Follow-Up After Section

The patients required follow-up examinations after hepatectomy for every 3–6 months, including serum tumor marker levels, abdominal ultrasonography, and contrast-enhanced CT or MRI. Recurrence was defined in cases of unequivocal new tumors observed by CT/MRI, PET-CT, or pathological confirmation. The interval from the date of surgery to the date of the first tumor recurrence, metastasis, or last follow-up was defined as recurrence-free survival (RFS), and overall survival (OS) was the interval between surgical resection and death or the last follow-up.

Statistical Analysis

Statistical analyses were performed by using SPSS 26.0 (IBM). Age and tumor size were continuous variables and expressed as the mean ± standard deviation, while the remaining variables were categorical variables and expressed as numbers and percentages. Cohen's kappa statistics were calculated to estimate interobserver agreement (0.0–0.2, poor; 0.2–0.4, fair; 0.4–0.6, moderate; 0.6–0.8, substantial; 0.8–1.0, perfect). One-way analysis of variance and the chi-squared test or Fisher's exact test were applied for the comparison of categorical variables. The differences of RFS and OS after hepatectomy in patients grouped on the basis of pathological, clinical, and imaging characteristics were performed using Kaplan-Meier survival curves and Log rank tests. Multivariable Cox proportional hazards model was used to identify the independent prognostic effects. Differences with a P value less than 0.05 were considered statistically significant.

Results

Clinical Data

The clinical characteristics of the 432 patients (overall mean age, 57.27±10.92 years), including 337 men (mean age, 57.02±11.03 years) and 95 women (mean age, 58.18±10.57 years), are summarized in Table 1. The cHCC-CCA cohorts

Table 1 Clinical and Pathologic Characteristics of Study Patients

Variable	HCC	cHCC-CCA	iCCA	*P* value
Number	239	100	93	
Mean age (y) *	57.22±10.78	54.80±11.02	59.98±10.92	0.006
All patients				
Men	195 (81.6%)	74 (74%)	68 (73.1%)	0.134
Women	44 (18.4%)	26 (26%)	25 (26.9%)	
M:F ratio	195/44	37/13	68/25	
Mean nodule size (cm) *	4.04±2.95	3.82±2.82	4.35±2.23	0.416
Cause of cirrhosis				
Hepatitis B	207 (86.6%)	90 (90%)	80 (86%)	0.134
Hepatitis C	26 (10.9%)	6 (6%)	6 (6.5%)	
Alcoholism	6 (2.5%)	4 (4%)	7 (7.5%)	
Tumor location				
Left lobe	70 (29.3%)	28 (28%)	33 (35.5%)	
Right lobe	163 (68.2%)	70 (70%)	60 (64.5%)	
Caudate lobe	6 (2.5%)	2 (2%)	0	
Tumor maker value				
AFP (≥20ng/mL)	109 (45.6%)	54 (54%)	13 (14%)	< 0.001
CEA (≥5ng/mL)	19 (7.9%)	16 (16%)	13 (14%)	0.064
CA 19–9 (≥37ng/mL)	30 (12.6%)	24 (24%)	39 (41.9%)	< 0.001
Microvascular invasion	77 (30.8%)	34 (34%)	29 (31.2%)	0.001

Notes: Except where indicated, data are numbers of patients, with percentages in parentheses. *Data are means ± standard deviations.

Abbreviations: AFP, alpha fetoprotein; CEA, carcinoembryonic antigen; CA 19–9, carbohydrate antigen 19–9; cHCC-CCA, combined hepatocellular-cholangiocarcinoma; HCC, hepatocellular carcinoma; iCCA, intrahepatic cholangiocarcinoma.

was younger than the iCCA and HCC cohorts (P = 0.006). In all three groups, HBV was the most common cause of liver cirrhosis. CA19-9 ≥ 37 ng/mL was more frequent in iCCA cohorts than in cHCC-CCA or iCCA cohorts, while AFP ≥ 20 ng/mL was more frequent in HCC cohorts (all P < 0.001). The remaining clinical characteristics (such as sex, tumor size, cause of cirrhosis and tumor location) were not significantly different between the three groups (all P > 0.05).

MRI Features

The MRI features of the three groups are summarized in Table 2. Non-rim APHE, enhancing capsule, and nonperipheral washout as the major features, were significantly more common in HCC (92.5%, 84.9%, and 80.7%, respectively) than in cHCC-CCA and iCCA (P < 0.001). Rim APHE, delayed central enhancement, peripheral washout, and targetoid restriction as the targetoid mass features, were significantly more common in iCCA (77.4%, 74.2%, 26.9%, and 25.8%, respectively) than in cHCC-CCA and HCC (P < 0.001). In addition, fat in mass was significantly more common in HCC (18% vs 7% vs.1.1%, P < 0.001), whereas iCCA had a considerably higher frequency of liver surface retraction (39.8%) and corona enhancement (44.1%) (all P < 0.001). Peritumoral bile duct dilatation and tumors in the vein were significantly more common in cHCC-CCA and iCCA than in HCC (all P < 0.05). Of the ancillary imaging features favoring HCC, mosaic architecture was least frequently noted in iCCA (P = 0.003).

LI-RADS Categories

A total of 432 nodules were included in the final LI-RADS Classification, and there were LR-3 in 9 nodules, LR-4 in 12 nodules, LR-5 in 228 nodules, LR-M in 150 nodules, and LR-TIV in 33 nodules (Table 3). In total 81.2% (194 of 239) of

Table 2 Imaging Characteristics of Hepatic Tumors in Cirrhotic Liver at Gadolinium Diethylenetriamine Pentaacetic Acid–Enhanced MRI

Variable	HCC (n=239)	cHCC-CCA (n=100)	iCCA (n=93)	P value	Kappa Value
Major imaging features					
Nodule size				0.096	
<10mm	7 (2.9%)	5 (5%)	0		
10–19mm	32 (13.4%)	18 (18%)	9 (9.7%)		
≥20mm	200 (83.7%)	77 (77%)	84 (90.3%)		
Non-rim arterial phase hyperenhancement	221 (92.5%)	59 (59%)	21 (22.6%)	< 0.001	0.89
Non-peripheral washout	203 (84.9%)	56 (56%)	11 (11.8%)	< 0.001	0.88
Enhancing capsule	193 (80.7%)	53 (53%)	22 (23.7%)	< 0.001	0.88
Targetoid mass imaging features					
Rim arterial phase hyperenhancement	22 (9.2%)	49 (49%)	72 (77.4%)	< 0.001	0.90
Peripheral washout	5 (2.1%)	4 (4%)	25 (26.9%)	< 0.001	0.86
Delayed central enhancement	18 (7.5%)	29 (29%)	69 (74.2%)	< 0.001	0.87
Targetoid restriction	10 (4.2%)	24 (24%)	24 (25.8%)	< 0.001	0.87
Tumor in the vein	10 (4.2%)	11 (11%)	12 (12.9%)	0.022	0.89
Ancillary imaging features					
Mild-moderate T2 hyperintensity	226 (94.6%)	94 (94%)	87 (93%)	0.42	0.84
Restricted diffusion	234 (97.9%)	98 (98%)	88 (95%)	0.053	1.0
Nodule-in-nodule	9 (3.8%)	8 (8%)	2 (2.2%)	0.127	0.76
Mosaic	42 (17.6%)	25 (25%)	6 (6.5%)	0.002	0.90
Fat in mass, more than adjacent liver	33 (21.2%)	7 (7%)	1 (1.1%)	< 0.001	0.83
Blood products in mass	40 (16.7%)	15 (15%)	7 (7.5%)	0.196	0.86
Peritumoral biliary dilatation	17 (7.1%)	30 (30%)	27 (29%)	< 0.001	0.92
Liver surface retraction	35 (14.6%)	17 (17%)	37 (39.8%)	< 0.001	0.95
Corona enhancement	33 (13.8%)	23 (23%)	41 (44.1%)	< 0.001	0.84

Note: Data are numbers of lesions, with percentages in parentheses.
Abbreviations: cHCC-CCA, combined hepatocellular-cholangiocarcinoma; HCC, hepatocellular carcinoma; iCCA, intrahepatic cholangiocarcinoma.

Table 3 Results of LI-RADS Categorization of 432 Hepatic Tumors

Variable	LR-3	LR-4	LR-5	LR-M	LR-TIV	*P* value
All Tumors (n=432)						0
HCC	4 (1.7%)	5 (2.1%)	194 (81.2%)	26 (10.8%)	10 (4.2%)	
cHCC-CCA	4 (4%)	3 (3%)	29 (29%)	53 (53%)	11 (11%)	
iCCA	1 (1.1%)	4 (4.3%)	5 (5.4%)	71 (76.3%)	12 (12.9%)	

Notes: Data are numbers of lesions, with percentages in parentheses. P value was obtained from the comparison among HCC, cHCC-CCA, and iCCA. Liver Imaging Reporting and Data System (LI-RADS) categories are defined as LR-3 (intermediate probability of HCC), LR-4 (probably hepatocellular carcinoma [HCC]), LR-5 (definitely HCC), LR-M (probably malignant, not specific for HCC), and LR-TIV (nodule with definite tumor in the vein).
Abbreviations: HCC, hepatocellular carcinoma; cHCC-CCA, combined hepatocellular-cholangiocarcinoma; iCCA, intrahepatic cholangiocarcinoma.

HCCs, 29% (29 of 100) of cHCC-CCAs, and 5.4% (5 of 93) of iCCAs were classified as LR-5; and 10.8% of (26 of 239) of HCCs, 53% (53 of 100) of cHCC-CCAs, and 76.3% (71 of 93) of iCCAs were classified as LR-M. The sensitivity of LR-5 as a predictor of HCC was 81.2% (194 of 239) and the specificity was 82.3% (159 of 193). In contrast, the sensitivity of LR-M as a predictor of non-HCC (iCCAs and cHCC-CCAs) was 64.2% (124 of 193) and the specificity was 89.1% (213 of 239). Interobserver agreements for the LI-RADS categorization were substantial to perfect (kappa = 0.7–1.0) (Table 2).

OS and RFS Outcomes for Different Pathological Stratifications After Surgery

A total of 172 patients experienced recurrences during the follow-up. As shown in Figure 2, the median OS and RFS for HCC (68 and 38 months) were longest, followed by cHCC-CCAs (48 and 24 months) and iCCAs (40 and 28 months) (all $P < 0.05$). No significant differences in OS or RFS were found between cHCC-CCAs and iCCAs (both $P > 0.05$) (Figure 2). Univariable analyses showed that tumor size >30 mm, pathologic diagnosis of cHCC-CCA and iCCA, LR-M category and CA19-9 ≥37ng/mL were significantly associated with poor OS and RFS (all $P < 0.05$). In multivariable analysis, LR-M category (hazard ratio: 1.69 for RFS, 1.86 for OS, both $P < 0.05$) and tumor size > 30 mm (hazard ratio: 1.42 for RFS, 2.13 for OS, both $P < 0.05$) were independent predictors of poor OS and RFS; pathologic diagnosis (hazard ratio: 1.58, $P = 0.037$ for cHCC-CCA compared with HCC) only demonstrated independent correlation with RFS (Table 4).

OS and RFS Outcomes for LI-RADS Categories

The median OS and RFS times were significantly longer in tumors classified as LR-4 or 5 than those in LR-M (64 vs 48 months; 38 vs 22 months, both $P < 0.001$) (Figure 3).

With regards to HCC cohorts, the RFS differed between tumors classified as LR-4 or 5 and those in LR-M (38 vs 28 months, $P = 0.03$), whereas the differences in OS between them were not statistically significant (64 vs 47 months, $P = 0.06$). Moreover, with regards to iCCA cohorts and cHCC-CCA cohorts, there were no significant differences in RFS between the tumors classified as LR-4 or 5 and those in LR-M category (all $P > 0.05$). For cHCC-CCA patients with tumor larger than 30mm, the OS times of patients classified as LR-4 or LR-5 were longer than that of patients classified as LR-M. ($P = 0.026$).

For patients categorized as LR-M, the OS and RFS in cHCC-CCA group were similar to those in the iCCA group (all $P > 0.05$) but worse than those in the HCC group (all $P < 0.05$) (Figure 4). However, the OS and RFS for cHCC-CCAs classified as LR-4 or 5 (Figure 5) were not significantly poorer than those for HCCs and iCCAs (all $P > 0.05$). Furthermore, cHCC-CCAs classified as LR-M (Figure 6) had no notable differences in OS and RFS compared with iCCAs categorized as LR-M (all $P > 0.05$), but there were significant differences in RFS between them if the tumor size was more than 30 mm ($P = 0.002$) (Figure 4).

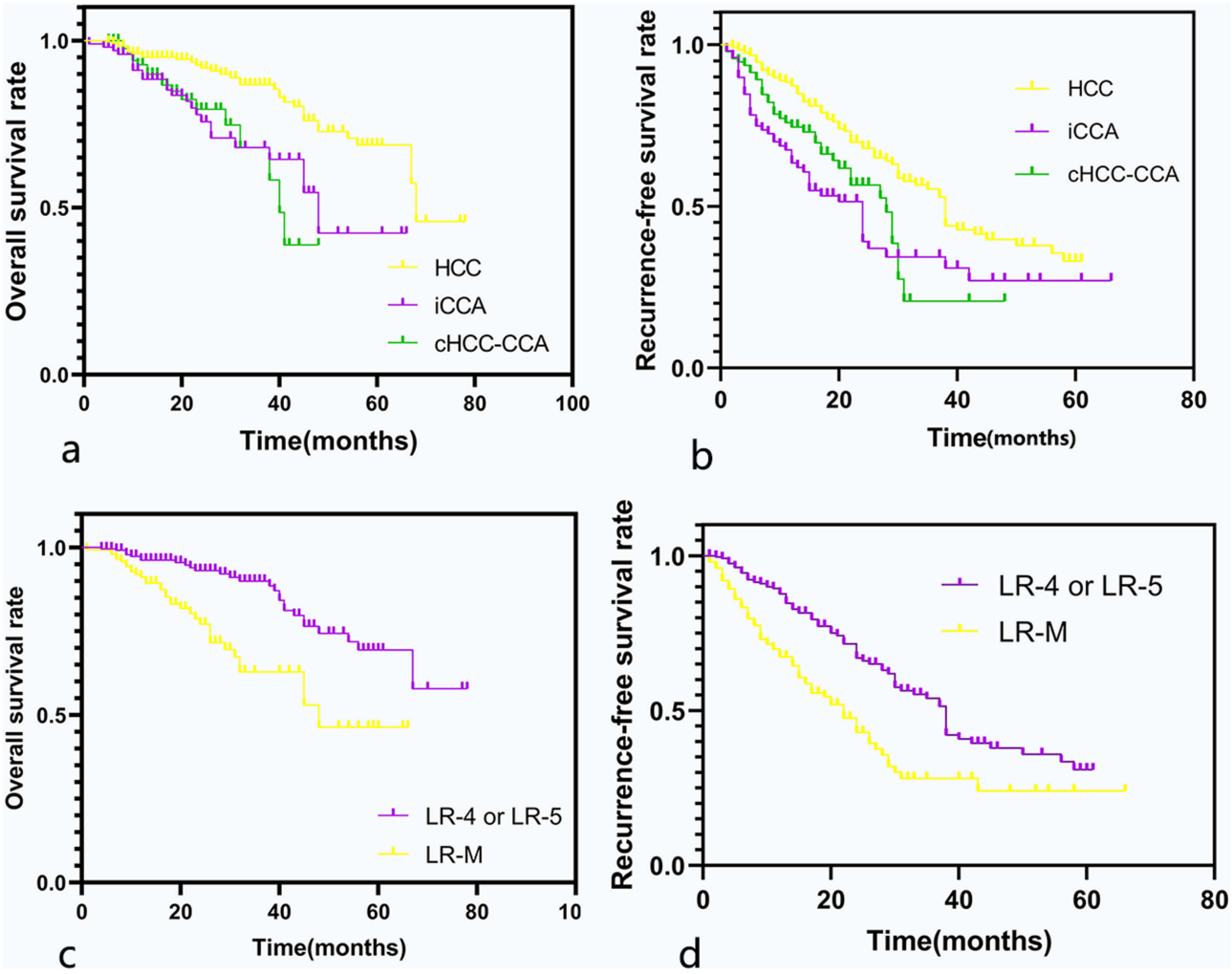

Figure 2 Recurrence-free survival and overall survival of 432 patients after surgical resection of primary liver cancer according to the Liver Imaging Reporting and Data System (LI-RADS) category and pathologic diagnosis. (**a** and **b**) Kaplan–Meier curves for overall survival (**a**) and recurrence-free survival (**b**) for patients with HCC, iCCA and HCC-CC. (**c** and **d**) Kaplan–Meier curves for overall survival (**c**) and recurrence-free survival (**d**) in the LR-M and LR-4/5 categories.
Abbreviations: cHCC-CCA, combined hepatocellular carcinoma-cholangiocarcinoma; HCC, hepatocellular carcinoma; iCCA, intrahepatic cholangiocarcinoma.

Prognostic Imaging Feature Predictors Between HCC and Non-HCC Malignancies

The univariable analysis revealed that non-rim APHE, nonperipheral washout, enhancing capsule, rim APHE, delayed central enhancement, corona enhancement, blood products in mass, mosaic architecture, peritumoral bile duct dilatation, and tumor in the vein were significantly associated with OS (all $P < 0.05$). Furthermore, the multivariable Cox analysis identified rim APHE (hazard ratio: 2.929, $P = 0.04$) and corona enhancement (hazard ratio: 1.784, $P = 0.032$) as independent determinants of poor OS in patients with primary liver cancers (Table 5). The survival analysis showed that non-rim APHE, nonperipheral washout, rim APHE, targetoid diffusion restriction, blood products in mass, peritumoral bile duct dilatation and Surface retraction were significantly associated with RFS (all $P < 0.05$). Nevertheless, the multivariable Cox regression analysis revealed that rim APHE (hazard ratio:2.322, $P = 0.019$) was independently correlated with poor RFS of PLC patients with cirrhosis. (Table 5).

Discussion

In this study, we evaluated the efficacy of LI-RADS 2018 at extracellular agent-enhanced MRI in the differential diagnosis of patients at risk for HCC in clinical practice. Our results showed that the specificity of the LR-5 category was 82.3% for differentiating HCCs from the PLCs, falling in the range between differentiating HCCs from iCCAs and

Table 4 Univariable and Multivariable Analyses of Clinical Factors Affecting Overall Survival and Recurrence-Free Survival

Variable	Overall Survival		Recurrence-Free Survival	
	Univariable Analysis	Multivariable Analysis	Univariable Analysis	Multivariable Analysis
Age	1.020(0.999, 1.042)[0.068]		0.999(0.985, 1.013)[0.895]	
Sex	1.021(0.595, 1.750)[0.941]		0.933(0.655, 1.330)[0.703]	
HBV	0.731(0.309, 1.731)[0.476]		1.254(0.675, 2.329)[0.474]	
AFP (≥20ng/mL)	1.156(0.737, 1.813)[0.528]		1.024(0.755, 1.388)[0.879]	
CEA (≥5ng/mL)	1.546(0.834, 2.869)[0.167]		1.293(0.839, 1.991)[0.244]	
CA 19–9 (≥37ng/mL)	2.212(1.349, 3.629)[0.002]		1.658(1.171, 2.347)[0.004]	
Tumor size (>3cm)	1.988(1.210, 3.264)[0.007]	2.131(1.241, 3.659)[0.006]	1.392(1.022, 1.895)[0.036]	1.429(1.034, 1.975)[0.031]
Pathologic diagnosis				
cHCC-CCA	2.551(1.504, 4.326)[0.001]		2.094(1.476, 2.973) [<0.01]	1.580(1.029, 2.427)[0.037]
iCCA	2.649(1.451, 4.835)[0.002]		1.702(1.151, 2.518)[0.008]	1.119(0.665, 1.884)[0.671]
HCC	1		1	
* LI-RADS category				
LR-4 or LR-5	1			
LR-M	2.595(1.580, 4.264)[<0.01]	1.869(1.002, 3.486)[0.049]	1.962(1.431, 2.691)[<0.01]	1.698(1.143, 2.522)[0.009]

Notes: Data are hazard ratios. Numbers in parentheses are 95% confidence intervals, and numbers in brackets are *P* values. *LI-RADS categories were defined as LR-4 (probably HCC), LR-5 (definitely HCC), and LR-M (probably malignant, not specific for HCC).

Abbreviations: cHCC-CCA, combined hepatocellular-cholangiocarcinoma; HCC, hepatocellular carcinoma; iCCA, intrahepatic cholangiocarcinoma; AFP, alpha fetoprotein; CEA, carcinoembryonic antigen; CA 19–9, carbohydrate antigen 19–9.

cHCC-CCAs (95% vs 71%). These results were in line with prior investigations using LI-RADS 2014 and 2017[2,3,10] but were not as high as desired. The first reason may be the special pathological properties of biphenotypic tumor, recent studies[23,24] demonstrated that the specificity of the LR-5 criterion was lowered by cHCC-CCA, which mimics HCC. Second, when hepatobiliary phase images were added, as shown by Min et al[16] the specificities of the LR-5 criterion were comparable (ECA-MRI,87.5%; HBA-MRI, 91.7%). In addition, our results were similar to those of Kim et al[17] using gadoxetate disodium contrast agent and LR2018 criteria: LR-M has reasonable specificity in differentiating non-HCC (iCCA and cHCC-CCA) from HCC. The specificity increased slightly compared to that in recent studies using the LR2017[10] or LR2014 criteria.[24] Intriguingly, the specificity of using LR-4/5 for diagnosing HCC did not significantly increase compared with LR-5, possibly due to the rarity of tumors ≤10 mm in our study compared with that in prior studies.[2,3,25] The updated LI-RADS 2018 version performed similarly to the 2017 version in diagnostic specificity for HCC, but increased the specificity of the LR-M category for non-HCC malignancies in patients with liver cirrhosis.

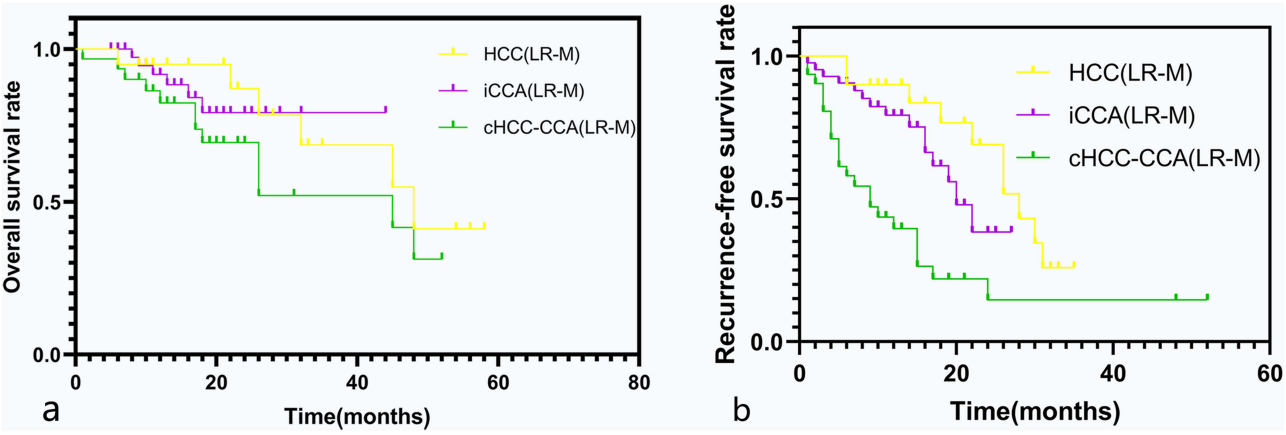

Figure 3 Recurrence-free survival and overall survival in patients with single primary liver cancer categorized as LR-M with tumor size >30 mm. Kaplan–Meier curves for overall survival (**a**) and recurrence-free survival (**b**) in LR-M with tumor size >30 mm according to pathologic diagnosis.

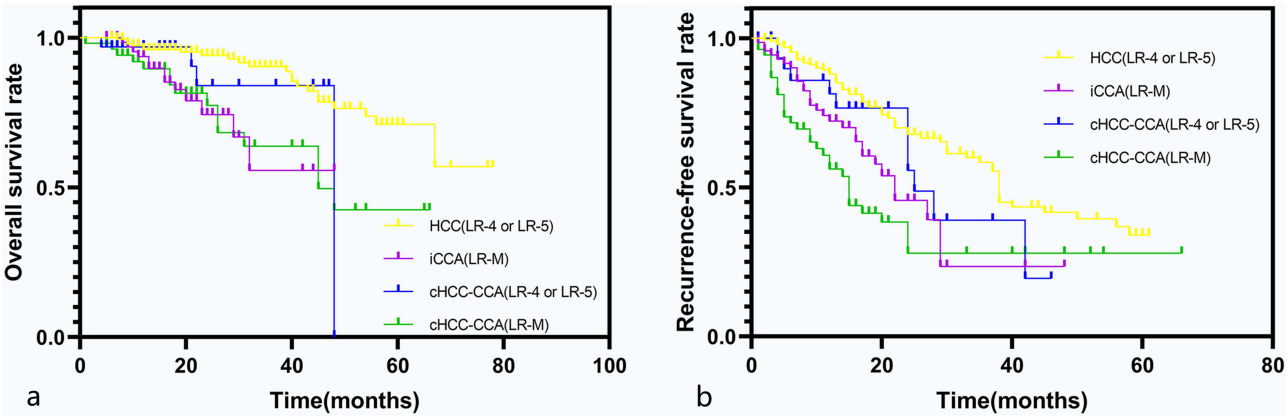

Figure 4 Recurrence-free survival and overall survival in patients with combined hepatocellular carcinoma-cholangiocarcinoma (cHCC-CCA) according to the Liver Imaging Reporting and Data System (LI-RADS) category in comparison with patients categorized as LR-4/5 with hepatocellular carcinoma (HCC) and patients categorized as LR-M with intrahepatic cholangiocarcinoma (iCCA). Kaplan–Meier curves show (**a**) overall survival and (**b**) recurrence-free survival after surgical resection of primary liver cancer.

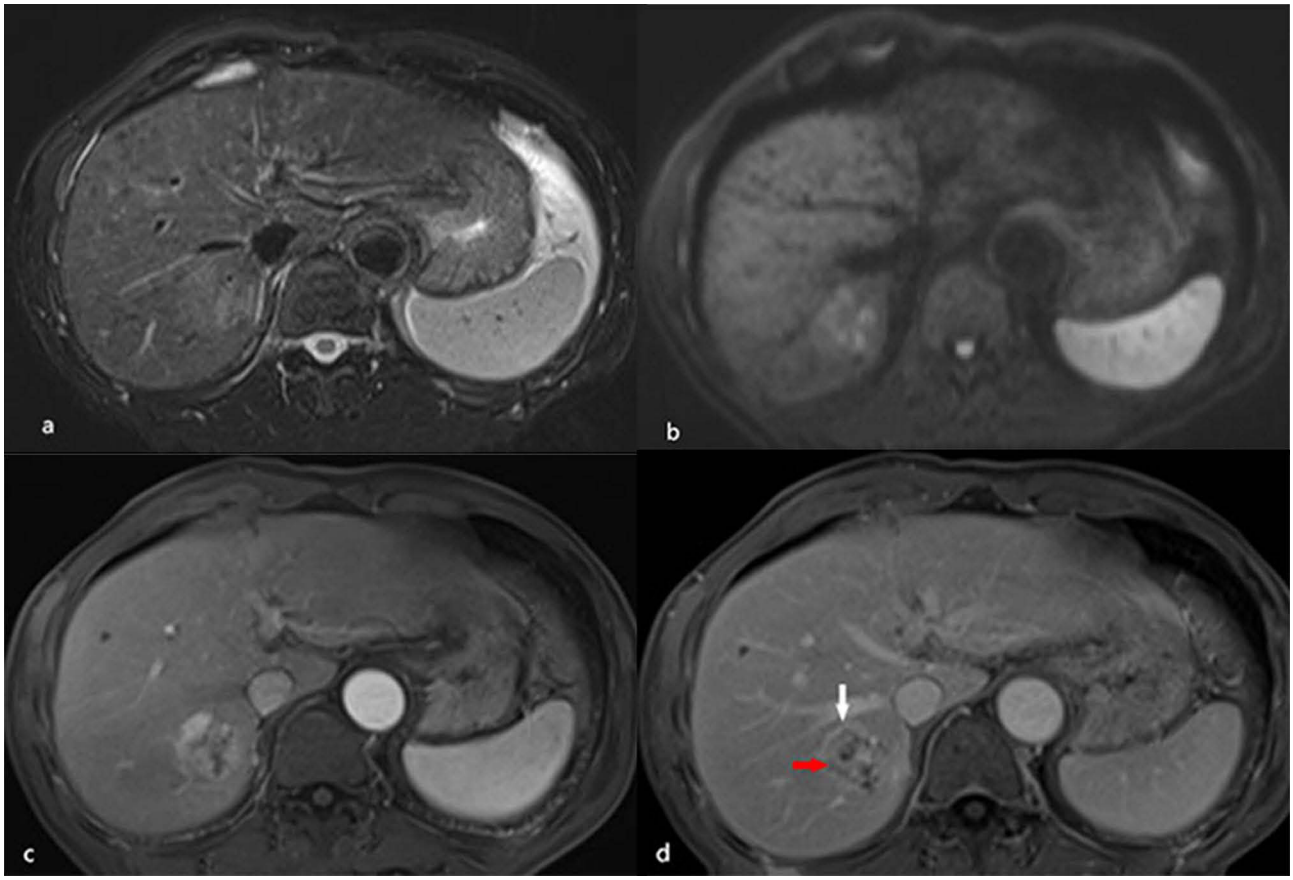

Figure 5 A 64-year-old male patient with hepatitis B–related liver cirrhosis and cHCC-CCA is categorized as Liver Imaging Reporting and Data System category LR-M. A 3.5 cm tumor in the right lobe of the liver shows heterogeneous hyperintensity on T2-weighted imaging (**a**) and diffusion weighted imaging (**b**). (**c**) The arterial phase shows peripheral enhancement on contrast-enhanced T1-weighted imaging with the contrast agent Gd-DTPA, and the nodule exhibits peripheral washout (red arrow) and an enhancing capsule (white arrow) in the delayed phase (**d**). Small recurrent lesions were found 5 months after surgery in this patient.

We also explored the relationship between pathological diagnosis and LI-RADS classification for postoperative prognosis in patients with liver cirrhosis. Primary liver cancers are considered a highly malignant disease because of their histologic and prognostic diversity.[10,26] Not surprisingly, the prognosis of cHCC-CCA, which shows variable biological behaviors and imaging features,[18,27,28] is most controversial.[29–31] Consistent with Tang et al[30] we found that the

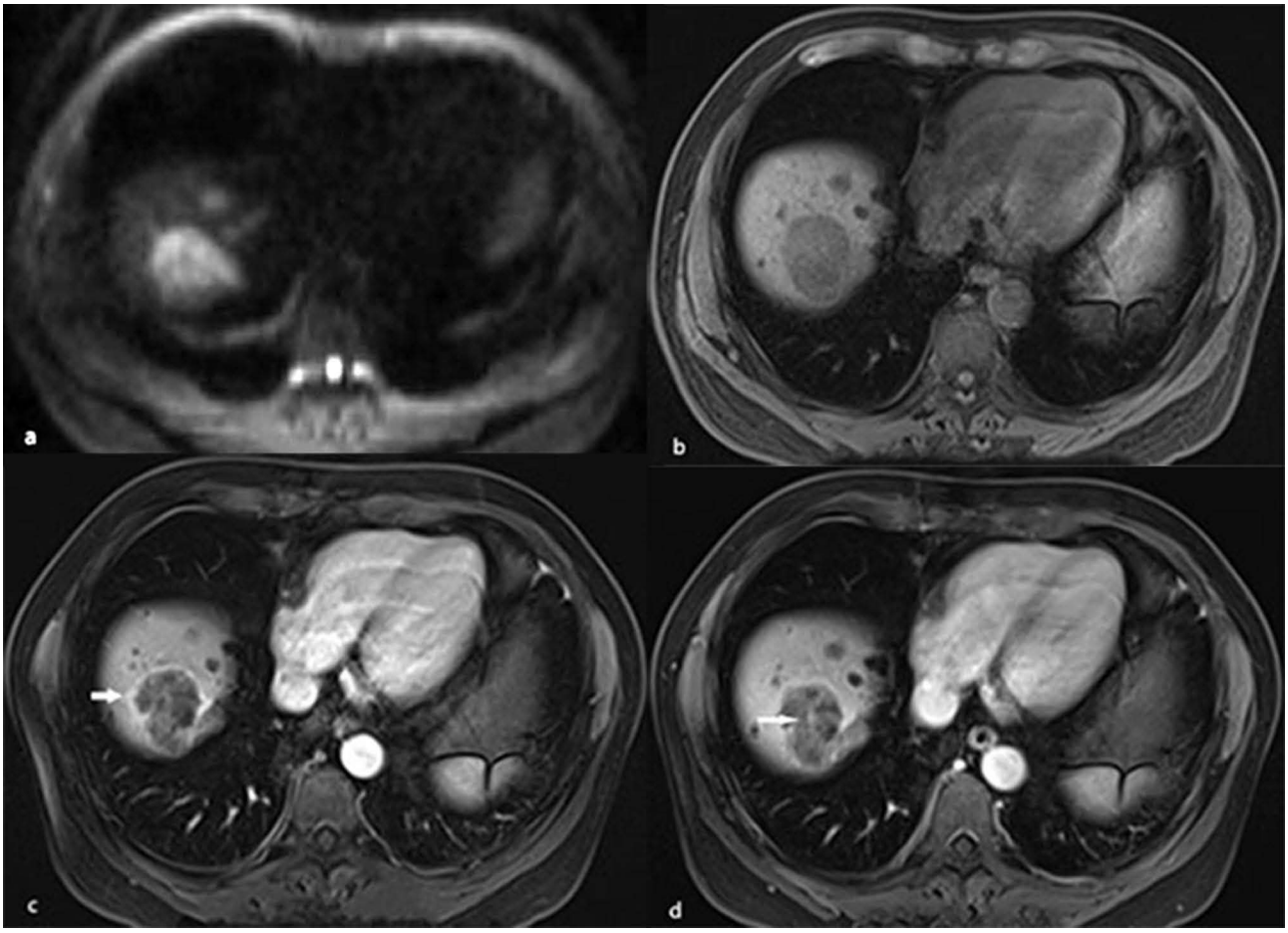

Figure 6 A 54-year-old male patient with hepatitis B–related liver cirrhosis and HCC is categorized as LR-M category. A 40-mm nodule shows heterogeneous hyperintensity on (**a**) diffusion weighted imaging. (**b**) T1-weighted imaging shows heterogeneous hypointensity in hepatic segment VIII. It presents rim arterial phase hyperenhancement (arrow) on contrast enhanced T1-weighted imaging (**c**) with contrast agent Gd-DTPA, resulting in delayed central enhancement (arrow) in (**d**) the delayed phase.

prognosis of HCCs was better than that of non-HCC malignancies.[32] The prognosis of cHCC-CCAs was worse than that of HCCs, yet similar to that of iCCAs, because major biliary tract invasion was more frequent in cHCC-CCAs and iCCAs that in HCCs.[30] Furthermore, we demonstrated that the RFS rate of cHCC-CCAs was lower than that of iCCAs,

Table 5 Univariable and Multivariable Analyses of Imaging Features Affecting Overall Survival and Recurrence-Free Survival

Variable	Overall Survival	Multivariable Analysis	Recurrence-Free Survival	Multivariable Analysis
	Univariable Analysis		Univariable Analysis	
Tumor size (>3cm)	1.988(1.210, 3.264)[0.007]	1.816(1.023, 3.224)[0.042]	1.392(1.022, 1.895)[0.036]	
Pathologic diagnosis				
cHCC-CCA	2.551(1.504, 4.326)[0.001]		2.094(1.476, 2.973) [<0.01]	1.802(1.182, 2.746)[0.006]
iCCA	2.649(1.451, 4.835)[0.002]		1.702(1.151, 2.518)[0.008]	1.382(0.809, 2.361)[0.236]
HCC	1		1	
Non rim arterial phase hyperenhancement	0.441(0.278, 0.699)[0.001]		0.586(0.429, 0.801)[0.001]	
Nonperipheral washout	0.483(0.306, 0.761)[0.002]		0.701(0.516, 0.951)[0.022]	
Enhancing capsule	0.490(0.311, 0.773)[0.002]		0.981(0.719, 1.340)[0.906]	
Rim arterial phase hyperenhancement	2.928(1.853, 4.627)[<0.01]	2.929(1.053, 8.149)[0.040]	1.947(1.435, 2.642)[<0.01]	2.322(1.148, 4.697)[0.019]
Peripheral washout	1.925(0.876, 4.229)[0.103]		1.286(0.729, 2.271)[0.385]	
Delayed central enhancement	1.962(1.206, 3.192)[0.007]		1.323(0.949, 1.846)[0.099]	
Targetoid restriction	1.358(0.746, 2.471)[0.317]		1.798(1.235, 2.617)[0.002]	

(*Continued*)

Table 5 (Continued).

Variable	Overall Survival	Multivariable Analysis	Recurrence-Free Survival	Multivariable Analysis
	Univariable Analysis		Univariable Analysis	
Tumor in the vein	2.600(1.398, 4.834)[0.003]		1.091(0.620, 1.921)[0.763]	
Nodule-in-nodule	0.712(0.221, 2.292)[0.569]		1.780(0.904, 3.504)[0.095]	
Mosaic	2.020(1.199, 3.403)[0.008]		1.322(0.896, 1.952)[0.159]	
Fat in mass, more than adjacent liver	0.498(0.227, 1.1.091)[0.082]		0.900(0.575, 1.410)[0.646]	
Blood products in mass	1.779(1.046, 3.028)[0.034]		1.520(1.040, 2.224)[0.031]	
Peritumoral biliary dilatation	1.758(1.034, 2.990)[0.037]		1.466(1.015, 2.117)[0.041]	
Liver surface retraction	1.034(0.596, 1.793)[0.905]		1.488(1.053, 2.103)[0.024]	
Corona enhancement	2.850(1.799, 4.513)[<0.01]	1.784(1.052, 3.027)[0.032]	1.264(0.895, 1.786)[0.183]	
Mild-moderate T2 hyperintensity	1.070(0.336, 3.402)[0.909]		2.230(0.827, 6.014)[0.113]	
Restricted diffusion	0.048(0.00, 24.363)[0.339]		1.607(0.512, 5.041)[0.416]	

Notes: Data are hazard ratios. Numbers in parentheses are 95% confidence intervals, and numbers in brackets are *P* values.
Abbreviations: cHCC-CCA, combined hepatocellular-cholangiocarcinoma; HCC, hepatocellular carcinoma; iCCA, intrahepatic cholangiocarcinoma; LI-RADS, Liver Imaging Reporting and Data System.

and the OS rate of cHCC-CCAs was higher than that of iCCAs. This result was in line with that of Takamichi,[31] which could be explained by the fact that cHCC-CCA was probably similar to HCC and had a better response to treatment in terms of recurrence.[33–35]

Similarly, as several studies reported,[10] the LI-RADS categories showed significant associations with OS and RFS and enabled the classification of patients with PLC according to their prognosis. The result in our study showed that tumors classified as LR-M had notably poorer OS and RFS than tumors classified as LR-4/5. In line with previous research findings,[10,29,36] the LI-RADS categories separated the classification of HCCs and cHCC-CCAs based on their postsurgical prognosis. We found that LR-4/5 cohorts had a relatively better RFS than LR-M cohorts in HCC patients and better OS in cHCC-CCAs patients with tumor size > 30 mm. Both cHCC-CCAs and iCCAs in LR-M had notably poorer OS and RFS than HCCs. This result was consistent with that of Choi et al[10] Interestingly, our study demonstrated that the LI-RADS categorization could also help distinguish the three pathological groups in tumors classified as LR-M according to their postsurgical prognosis under certain conditions. cHCC-CCAs categorized as LR-M had a significantly poorer OS than HCCs in the same category and a significantly poorer RFS than iCCAs in the same category in patients with tumor sizes > 30 mm. The main reason for this result was that tumor size > 30 mm in our study was an independent prognostic factor for poor OS and RFS, while Yoon et al[29] demonstrated unanimous results in patients with cHCC-CCA. Lu et al[37] demonstrated that the 3 cm cutoff seems to best determine the biological behavior and clinical prognosis of patients undergoing partial hepatectomy for early stage HCC.

Therefore, the LI-RADS category, which contains these known prognostic imaging characteristics, is a standardized and comprehensive categorization system for hepatic nodules in high-risk patients, and can also be regarded as a prognostic imaging biomarker for PLCs.[8] With this background, replaced with our research individually analyzed the prognostic value of the most known LI-RADS imaging features to stratify PLCs according to their prognosis.[10,11,25] As previously reported,[7,36,38] our study demonstrated that the major features as favorable prognostic features were not independent predictors of OS and RFS. In contrast, rim APHE for the targetoid mass features and corona enhancement for the ancillary imaging features were significantly correlated with poor prognosis. The results were also supported by most previous studies, which reported that rim APHE was the most sensitive imaging feature for identifying non-HCC malignancies (iCCA and cHCC-CCA) in the LI-RADS target observations. Wang et al[18] identified that corona enhancement and delayed central enhancement as predictors of RFS in cHCC-CCA patients categorized as LR-M, and mosaic architecture as predictors of RFS in cHCC-CCA patients categorized as LR-4/5. The findings in our study of PLCs were slightly different from those of cHCC-CCAs. Therefore, clinicians can evaluate each patient's prognosis simply by counting the number of identified risk factors.

Our study had several limitations. First, the retrospective design of our investigation could lead to selection bias, this study did not include benign lesions in the assessment of diagnostic performance, and only included iCCA and cHCC-

CCA lesions as non-HCC malignancies in cirrhotic livers, in which the proportions of iCCAs and cHCC-CCAs were overestimated compared with the actual incidence of cirrhosis. Second, our study only included solitary masses in patients with PLCs with Child–Pugh A class that were surgically resected. Finally, our results were obtained from the diagnostic consensus of two very experienced radiologists and may not fully account for interdiagnostic differences in LI-RADS classifications.

In conclusion, the LI-RADS categories can predict the postsurgical prognosis of primary liver cancers independently.

Abbreviations

PLC, Primary liver cancer; HCC, Hepatocellular Carcinoma; iCCA, Intrahepatic cholangiocarcinoma; cHCC-CCA, combined hepatocellular carcinoma-cholangiocarcinoma; LI-RADS, Liver Imaging Reporting and Data System; ECA, extracellular contrast agents; HBA, hepatobiliary agents; AFP, alpha-fetoprotein; CEA, carcinoembryonic antigen; CA 19-9, carbohydrate antigen 19-9; Gd-DTPA, gadolinium diethylenetriamine pentaacetic acid; APHE, arterial phase hyperenhancement; CCA, cholangiocarcinoma; RFS, recurrence-free survival; OS, overall survival.

Funding

This study was supported by Clinical Research Plan of SHDC (grant number SHDC2020CR1029B), National Natural Science Foundation of China (grant number 82171897), Shanghai Municipal Key Clinical Specialty (grant number shslczdzk03202), Clinical Research Project of Zhongshan Hospital, Fudan University (grant number 2020ZSLC61), Henan Provincial Universities Key scientific research projects (grant number 21B320002).

Disclosure

The authors report no conflicts of interest in this work.

References

1. Petrick JL, Kelly SP, Altekruse SF, McGlynn KA, Rosenberg PS. Future of hepatocellular carcinoma incidence in the United States forecast through 2030. *J Clin Oncol*. 2016;34(15):1787–1794. doi:10.1200/JCO.2015.64.7412
2. Kierans AS, Makkar J, Guniganti P, et al. Validation of liver imaging reporting and data system 2017 (LI-RADS) criteria for imaging diagnosis of hepatocellular carcinoma. *J Magn Reson Imaging*. 2019;49(7):e205–e15.
3. van der Pol CB, Lim CS, Sirlin CB, et al. Accuracy of the liver imaging reporting and data system in computed tomography and magnetic resonance image analysis of hepatocellular carcinoma or overall malignancy-A systematic review. *Gastroenterology*. 2019;156(4):976–986.
4. Choi SH, Lee SS, Kim SY, et al. Intrahepatic cholangiocarcinoma in patients with cirrhosis: differentiation from hepatocellular carcinoma by using gadoxetic acid-enhanced MR imaging and dynamic CT. *Radiology*. 2017;282(3):771–781.
5. Kim HD, Lim YS, Han S, et al. Evaluation of early-stage hepatocellular carcinoma by magnetic resonance imaging with gadoxetic acid detects additional lesions and increases overall survival. *Gastroenterology*. 2015;148(7):1371–1382.
6. Garancini M, Goffredo P, Pagni F, et al. Combined hepatocellular-cholangiocarcinoma: a population-level analysis of an uncommon primary liver tumor. *Liver Transpl*. 2014;20(8):952–959.
7. Jiang H, Song B, Qin Y, et al. Diagnosis of LI-RADS M lesions on gadoxetate-enhanced MRI: identifying cholangiocarcinoma-containing tumor with serum markers and imaging features. *Eur Radiol*. 2021;31(6):3638–3648.
8. Elsayes KM, Hooker JC, Agrons MM, et al. 2017 Version of LI-RADS for CT and MR Imaging: an Update. *RadioGraphics*. 2017;37(7):1994–2017.
9. Chernyak V, Fowler KJ, Kamaya A, et al. Liver imaging reporting and data system (LI-RADS) Version 2018: imaging of hepatocellular carcinoma in at-risk patients. *Radiology*. 2018;289(3):816–830.
10. Choi SH, Lee SS, Park SH, et al. LI-RADS classification and prognosis of primary liver cancers at gadoxetic acid-enhanced MRI. *Radiology*. 2019;290(2):388–397.
11. Lee S, Kim SS, Chang DR, Kim H, Kim MJ. Comparison of LI-RADS 2018 and KLCA-NCC 2018 for noninvasive diagnosis of hepatocellular carcinoma using magnetic resonance imaging. *Clin Mol Hepatol*. 2020;26(3):340–351.
12. Hope TA, Fowler KJ, Sirlin CB, et al. Hepatobiliary agents and their role in LI-RADS. *Abdom Imaging*. 2015;40(3):613–625.
13. Chanyaputhipong J, Low SC, Chow PK. Gadoxetate acid-enhanced MR Imaging for HCC: a review for clinicians. *Int J Hepatol*. 2011;2011:489342.
14. Tamada T, Ito K, Sone T, et al. Dynamic contrast-enhanced magnetic resonance imaging of abdominal solid organ and major vessel: comparison of enhancement effect between Gd-EOB-DTPA and Gd-DTPA. *J Magn Reson Imaging*. 2009;29(3):636–640.
15. Vogl TJ, Kümmel S, Hammerstingl R, et al. Liver tumors: comparison of MR imaging with Gd-EOB-DTPA and Gd-DTPA. *Radiology*. 1996;200(1):59–67.
16. Min JH, Kim JM, Kim YK, et al. Prospective intraindividual comparison of magnetic resonance imaging with gadoxetic acid and extracellular contrast for diagnosis of hepatocellular carcinomas using the liver imaging reporting and data system. *Hepatology*. 2018;68(6):2254–2266.

17. Davenport MS, Viglianti B, Al-Hawary MM, et al. Comparison of acute transient dyspnea after intravenous administration of gadoxetate disodium and gadobenate dimeglumine: effect on arterial phase image quality. *Radiology*. 2013;266(2):452–461.
18. Wang Y, Zhu G-Q, Zhou C-W, Li N, Yang C, Zeng M-S. Risk stratification of LI-RADS M and LI-RADS 4/5 combined hepatocellular cholangiocarcinoma: prognostic values of MR imaging features and clinicopathological factors. *European Radiology*. 2022;32(8):5166–5178.
19. Hwang J, Kim YK, Min JH, et al. Capsule, septum, and T2 hyperintense foci for differentiation between large hepatocellular carcinoma (>/=5 cm) and intrahepatic cholangiocarcinoma on gadoxetic acid MRI. *Eur Radiol*. 2017;27(11):4581–4590.
20. Choi SY, Kim YK, Min JH, et al. Added value of ancillary imaging features for differentiating scirrhous hepatocellular carcinoma from intrahepatic cholangiocarcinoma on gadoxetic acid-enhanced MR imaging. *Eur Radiol*. 2018;28(6):2549–2560.
21. Huang P, Zhou C, Wu F, et al. An improved diagnostic algorithm for subcentimeter hepatocellular carcinoma on gadoxetic acid-enhanced MRI. *European Radiology*. 2020;2020:1432. doi:10.1007/s00330-022-09282-5
22. Nagtegaal ID, Odze RD, Klimstra D, et al. The 2019 WHO classification of tumours of the digestive system. *Histopathology*. 2020;76:1365–2559.
23. Kim -Y-Y, Kim M-J, Kim EH, Roh YH, An C. Hepatocellular carcinoma versus other hepatic malignancy in cirrhosis: performance of LI-RADS version 2018. *Radiology*. 2019;291(1):72–80.
24. Fraum TJ, Tsai R, Rohe E, et al. Differentiation of hepatocellular carcinoma from other hepatic malignancies in patients at risk: diagnostic performance of the liver imaging reporting and data system version 2014. *Radiology*. 2018;286(1):158–172.
25. Kim YY, An C, Kim S, Kim MJ. Diagnostic accuracy of prospective application of the Liver Imaging Reporting and Data System (LI-RADS) in gadoxetate-enhanced MRI. *Eur Radiol*. 2018;28(5):2038–2046.
26. Choi SY, Kim SH, Park CK, et al. Imaging features of gadoxetic acid-enhanced and diffusion-weighted MR imaging for identifying cytokeratin 19-positive hepatocellular carcinoma: a retrospective observational study. *Radiology*. 2018;286(3):897–908.
27. Joseph NM, Tsokos CG, Umetsu SE, et al. Genomic profiling of combined hepatocellular-cholangiocarcinoma reveals similar genetics to hepatocellular carcinoma. *J Pathol*. 2019;248(2):164–178.
28. Xue R, Chen L, Zhang C, et al. Genomic and transcriptomic profiling of combined hepatocellular and intrahepatic cholangiocarcinoma reveals distinct molecular subtypes. *Cancer Cell*. 2019;35(6):932–47 e8.
29. Yoon J, Hwang JA, Lee S, Lee JE, Ha SY, Park YN. Clinicopathologic and MRI features of combined hepatocellular-cholangiocarcinoma in patients with or without cirrhosis. *Liver Int*. 2021;41(7):1641–1651.
30. Tang Y, Wang L, Teng F, Zhang T, Zhao Y, Chen Z. The clinical characteristics and prognostic factors of combined hepatocellular carcinoma and cholangiocarcinoma, hepatocellular carcinoma and intrahepatic cholangiocarcinoma after surgical resection: a propensity score matching analysis. *Int J Med Sci*. 2021;18(1):187–198.
31. Ishii T, Ito T, Sumiyoshi S, et al. Clinicopathological features and recurrence patterns of combined hepatocellular-cholangiocarcinoma. *World J Surg Oncol*. 2020;18(1):319.
32. Chu KJ, Lu CD, Dong H, Fu XH, Zhang HW, Yao XP. Hepatitis B virus-related combined hepatocellular-cholangiocarcinoma: clinicopathological and prognostic analysis of 390 cases. *Eur J Gastroenterol Hepatol*. 2014;26(2):192–199.
33. Zhou YM, Sui CJ, Zhang XF, Li B, Yang JM. Influence of cirrhosis on long-term prognosis after surgery in patients with combined hepatocellular-cholangiocarcinoma. *BMC Gastroenterol*. 2017;17(1):25.
34. Ludwig DR, Fraum TJ, Cannella R, et al. Hepatocellular carcinoma (HCC) versus non-HCC: accuracy and reliability of liver imaging reporting and data system v2018. *Abdom Radiol*. 2019;44(6):2116–2132.
35. Fraum TJ, Cannella R, Ludwig DR, et al. Assessment of primary liver carcinomas other than hepatocellular carcinoma (HCC) with LI-RADS v2018: comparison of the LI-RADS target population to patients without LI-RADS-defined HCC risk factors. *Eur Radiol*. 2020;30(2):996–1007.
36. Wang X, Wang W, Ma X, et al. Combined hepatocellular-cholangiocarcinoma: which preoperative clinical data and conventional MRI characteristics have value for the prediction of microvascular invasion and clinical significance? *Eur Radiol*. 2020;30(10):5337–5347.
37. Lu XY, Xi T, Lau WY, et al. Pathobiological features of small hepatocellular carcinoma: correlation between tumor size and biological behavior. *J Cancer Res Clin Oncol*. 2011;137(4):567–575.
38. Zhou C, Wang Y, Ma L, Qian X, Yang C, Zeng M. Combined hepatocellular carcinoma-cholangiocarcinoma: MRI features correlated with tumor biomarkers and prognosis. *Eur Radiol*. 2022;32(1):78–88.